Egyptian Journal of Chemistry

http://ejchem.journals.ekb.eg/

Bioactive Nanocomposite of Squash Mucilage, Selenium and Chitosan Nanoparticles as Potential Candidate for Diabetes Control

Hend A. Gad [1], Mahmoud A. Al-Saman [2], Shaaban H. Moussa [3]*, Ahmed A. Tayel [1]*

[1] Department of Fish Processing and Biotechnology, Faculty of Aquatic and Fisheries Sciences, Kafrelsheikh University, Kafrelsheikh 33516, Egypt

[2] Department of Industrial Biotechnology, Genetic Engineering and Biotechnology Research Institute, University of Sadat City, El-Sadat City, Egypt

[3] Department of Biology, College of Science and Humanitarian Studies, Shaqra University, Qwaieah 11971, Saudi Arabia

Abstract

The research investigates the potential of utilizing nanocomposites of squash mucilage (SqM), chitosan (Cht) and biogenic selenium (SeNPs) nanoparticles as nanocarriers for improving oral delivery of insulin and controlling diabetes. The research aims to explore the synthesis and characterization of these nanocomposites, evaluating their biocompatibility, stability, and encapsulation efficiency for insulin. The study further investigates the release kinetics of insulin from the SqM, SeNPs and Cht nanocomposites, assessing their ability to provide sustained and controlled release. The conjugation of SeNPs mediated by SqM with Cht for drug delivery purposes represents a promising strategy in pharmaceutical research. The interactions between molecules were validated with FTIR (infrared) analyses. The SqM/SeNPs had 13.46 nm mean diameter, with negative (- 28.61 mV) surface charges. Three nanoformulations from Cht/SqM/SeNPs were constructed (i.e. ILNs-1, ILNs-2, and ILNs-3), with 1:2, 1:1, 2:1 ratios, respectively. The average sizes of the nanocomposites were 395.93, 235.43 and 308.72 nm, whereas their surface charges were -26.41, -11.46 and +18.62 mV, respectively. The electron microscopy (TEM and SEM) confirmed the nanomaterials' homogenous structures and dispersion. The insulin encapsulation efficiency and loading capacity with ILNs-3 were 75.7% and 4.76%, respectively. The insulin release from ILNs-3 at different pH values (1.2 and 6.8) were 35% and 68%, respectively, after two hours. The in vivo pharmacological assessment demonstrated the effectual sustained action of ILNs-loaded insulin for lowering glucose levels up to 24 h of oral administration. This innovative approach develops the natural properties of SqM and the versatile characteristics of Cht to develop a biocompatible and effective carrier system. The synergistic interaction between these components opens new possibilities for the development of drug delivery systems with improved efficacy, reduced toxicity, and increased patient compliance.

Keywords: Biopolymers; nanocomposites; drug delivery; diabetes control; insulin

1. Introduction

Oral insulin administration represents a promising approach in the field of diabetes management, offering an alternative method to traditional insulin delivery methods such as injections [1]. The goal of oral insulin is to provide a more patient-friendly and convenient option for individuals with diabetes who require insulin supplementation [2]. One of the primary advantages of oral insulin is its potential to enhance patient compliance. Many individuals with diabetes may find injections inconvenient, leading to adherence challenges [3]. Oral administration eliminates the need for needles, making it a more accessible and acceptable option for a broader range of patients. This can be particularly beneficial for those with a fear of needles or discomfort associated with injections.

The development of oral insulin faces several challenges, primarily related to the digestive processes in the gastrointestinal tract. The gastrointestinal environment poses obstacles to the effective absorption of intact insulin molecules, as the digestive enzymes and acidic conditions can degrade insulin before it reaches the bloodstream [4]. To overcome these challenges, various formulation strategies, such as encapsulation and modification of insulin molecules, are being explored to protect insulin during its journey through the digestive system [5].

Nanotechnology plays a significant role in the development of oral insulin delivery systems. Nanoparticles and nanocarriers can protect insulin from degradation, enhance its absorption, and facilitate its transport across the intestinal epithelium [6]. These nanosystems can be designed to release insulin in a controlled manner, mim-

*Correspondences author: ahmed_tayel@fsh.kfs.edu.eg; ORCID: 0000-0001-9411-134X; shaaban@su.edu.sa

Received date 08 January 2025; **Revised date** 31 January 2025; **Accepted date** 09 February 2025

DOI: 10.21608/ejchem.2025.351451.11132

©2025 National Information and Documentation Centre (NIDOC)

icking the physiological insulin secretion pattern. Moreover, the use of absorption enhancers, permeation enhancers, and other formulation technologies aims to improve the bioavailability of oral insulin. Researchers are investigating innovative approaches to overcome the challenges associated with insulin stability, absorption, and therapeutic efficacy to make oral insulin a viable and effective option for diabetes management [7].

The most significant and rapidly advancing materials in science currently are metallic nanoparticles (NPs). Due to their extremely small size (in nm) and high surface-to-volume ratio, NPs have gathered excessive interest as they exhibit different physical and chemical properties from materials with a majority of the same chemical composition [8].

Selenium nanoparticles have versatile applications, drawing increased attention due to their large specific surface area, high surface activity, significant biological activity, along with high bioavailability and low toxicity [9]. Selenium (Se) has gained growing attention in recent years for its crucial role in maintaining human health [10, 11]. It is essential for various metabolic processes, including thyroid hormone metabolism and immunological responses. By being incorporated into antioxidant enzymes, it also prevents cellular damage caused by free radicals. Numerous serious disorders, such as cancer, cardiovascular, and inflammatory diseases, have been linked to Se deficiency [12]. However, toxicity may result from larger amounts or long-term Se administration [13].

Chitosan is a versatile biopolymer derived from chitin, which is abundantly found in the exoskeletons of crustaceans such as shrimp, crab, and other shellfish. It is considered one of the most promising natural polymers due to its unique properties and various applications in diverse fields, ranging from biomedical and pharmaceutical to food and agriculture [14]. Cht is a linear polysaccharide composed of repeating units of β-(1→4)-linked D-glucosamine and N-acetyl-D-glucosamine. It is utilized as a surface coating layer on nanoparticles to improve enzymatic, chemical, and mucoadhesive stability, given its possession of active amino and hydroxyl groups [15]. Studies on Cht modification for insulin delivery involve exploring various strategies to enhance the effectiveness of Cht-based carriers in delivering insulin. These modifications aim to improve factors such as stability, bioavailability, and controlled release of insulin. Some common approaches include chemical modifications, structural alterations, and the incorporation of other materials into Cht matrices. These studies contribute to the development of advanced drug delivery systems for improved therapeutic outcomes in diabetes management [15]. Cht has garnered significant attention in the development of novel bioadhesive drug delivery systems. Its unique properties make it an attractive material for formulating drug delivery systems that adhere to biological surfaces, providing sustained and targeted release of therapeutic agents [16]. By interacting with the negative charges present on mucosal surfaces, Cht has the ability to induce the redistribution of cytoskeletal F-actin and the tight junction protein ZO-1. This phenomenon leads to an elevation in the paracellular permeability of hydrophilic macromolecules [17].

Squash (*Cucurbita moschata*) is a versatile and nutritious fruit that belongs to the gourd family. It is widely recognized for its rich content of vitamins (e.g. A, C and B complex), diverse minerals, carotenes, and amino acids [18]. Beyond its culinary applications, squash has garnered attention in the field of drug delivery. The use of squash as a component in nanocarrier involves extracting mucilage from the fruit, primarily from its seeds and rind. Mucilage is a gelatinous substance found in various plant tissues, and in squash, it serves as a potential natural material for drug delivery applications. The mucilage extracted from squash contains polysaccharides, proteins, and other bioactive compounds that contribute to its adhesive and mucoadhesive properties [19]. When combined with Cht, the resulting nano-mucilage carrier exhibits enhanced functionality for drug delivery. Cht provides structural support, stability, and controlled release properties to the carrier system [20]. The combination of SqM and Cht offers the advantage of improved bioavailability and sustained release of therapeutic agents. Utilizing aqueous plant extracts presents a favorable alternative to chemical methods for nanoparticle production. This approach requires non-toxic solvents, mild temperatures, and readily available, cost-effective, biodegradable reducing agents that pose no harm to the environment. Due to its minimal toxicity towards living organisms such as plants, microalgae, and other environmental microbes, green synthesis nanoparticles emerge as a potential substitute for antibiotics [21]. This study aims to develop and evaluate novel nanocomposites composed of SqM, SeNPs, and Cht as nanocarriers for insulin delivery. The research focuses on assessing the release kinetics and stability of insulin from these nanopolymers, with an emphasis on achieving controlled and sustained drug release. Additionally, the study seeks to explore the biocompatibility and potential of these nanocomposites for improving the efficacy and safety of insulin delivery systems.

2. MATERIALS AND METHODS

2.1. Preparation of Squash (*Cucurbita moschata*) extract

Squash (*Cucurbita moschata*) was harvested at a comparable age and physical characteristics (e.g. average weight of 3.19±0.64 kg, bulb diameter of 42.68±3.41 cm, and external length of 53.91±6.13 cm) from the ARC

(Agriculture Research Centre) in Kafrelsheikh, Egypt. The fruits underwent a meticulous process where their thick peel layers were peeled, and the seeds were manually extracted. Subsequently, the fruits were sliced into thin slices and subjected to a three-day drying period at 40°C. Prior to drying, the fruits were thoroughly cleaned using flowing chlorinated water to eliminate any residual contaminants on the fruit's surface [22]. The dried fruits were then ground into powder, and the obtained powder was immersed in 15-fold distilled water for an entire day before undergoing filtration through a white muslin cloth.

2.1.1. Extraction of squash mucilage

The precipitation of mucilage was achieved by using 95% ethanol, with the amount of ethanol being twice that of the aqueous mixture [23]. Following this, the obtained mucilage was passed through a white muslin cloth and subsequently dried for 48 hours at approximately 42°C in an oven. The resulting mucilage from hard squash was then ground and stored in desiccators for future use [24].

2.2. Synthesis of Selenium Nanoparticles

In summary, 10 mL of an aqueous extract of SqM was slowly added drop by drop to 10 mL of 10 mM sodium selenite (Na_2SeO_3, Sigma-Aldrich, MO) under magnetic stirring conditions. Subsequently, the reaction mixture was left to undergo reduction in the dark at 27 ± 2°C and 120 rpm on an orbital shaker (Solaris 2000-R; Thermo Fisher Scientific Inc.) for 24 hours, with observations made for any color change [25]. To obtain clear SeNPs, the components of the SqM/SeNPs composition underwent centrifugation following each of the three washes with distilled water and the two washes with ethanol [26].

2.3. Preparation of Insulin Loaded biopolymer Nanocomposite (ILNs)

Chitosan flakes were dissolved in 50 mL of a 1% v/v aqueous acetic acid solution at room temperature for 8 hrs. Subsequently, 10 IU of insulin was added to 5 mL of 0.1% w/v chitosan solution, following by a 2 mL drop-by-drop addition of 0.1% w/v SqM/SeNPs solution took place at room temperature over 30 minutes. This process occurred while continuously stirring on a magnetic stirrer. The resulting reaction mixture underwent centrifugation at 15,000 rpm and 4°C for 50 minutes. After decanting the supernatant, the nanoparticles were re-suspended in sterile distilled water and subjected to a 15-min re-centrifugation at 15,000 rpm and 4°C to separate them [17].

2.4. Characterization of Insulin Loaded biopolymer Nanocomposites (ILNs)

2.4.1. Fourier Transform Infrared (FTIR) Spectroscopy

FTIR (Fourier-Transform Infrared) spectroscopy is a powerful analytical technique widely used for various applications due to its ability to provide valuable insights into the chemical composition and molecular structure of substances. The FTIR spectra (Model 4000, JASCO, Japan) were utilized to showcase the functional moieties and chemical interactions of the loaded Nanocomposites, spanning the range from 4000 to 450 cm^{-1} [15].

2.4.2. Zeta Potential (ζ) and particle size Analysis

After dissolving the ILNs, DLS (dynamic light scattering) and photon correlation spectroscopy were conducted using a Zetasizer (MalvernTM, UK) to analyze the size, surface charges, and distribution of the synthesized materials. Briefly, 1 mg/mL^{-1} of nanomaterials were dispersed in de-ionized water and subjected to 70 s of sonication at 40 W in an ice bath (Sonifier S250A, Branson Ultrasonics, Danbury, CT). Measurements were performed three times at R.T, and each experiment was assessed twice.

2.4.3. Transmission Electron Microscopy (TEM)

TEM plays a crucial role in providing detailed insights into the structure and morphology of ILN. By utilizing a high-energy electron beam, TEM allows for the visualization of nanoscale features with exceptional resolution. The technique involves transmitting electrons through the sample, and the resulting image provides information about the size which is vital for understanding the uniformity and effectiveness of the nanoparticle, shape, and distribution of the nanoparticles. The TEM "JEOL Ltd., JEM-1010, Tokyo, Japan" pictures of SqM/SeNPs were captured "at 200 kV" accelerated voltage, to review SeNPs structure and morphology. The nanomaterials' solution was dropped/casted and air-dried on TEM carbon grids, then screened.

2.4.4. Scanning Electron Microscopy (SEM) SEM is a valuable imaging technique that plays a crucial role in characterizing the surface morphology and structural features of insulin-loaded nanoparticles. Unlike traditional light microscopy, SEM uses electron beams to scan the surface of a sample, providing high-resolution, three-dimensional images. The SEM "JEOL, JSM IT100, Japan" was employed to characterize size, morphology and surface structure of nanocomposites after gold/palladium coating.

2.5. EE (Encapsulation Efficiency) and LD (Loading Degree) of Insulin

The Nanocomposites were dispersed in Phosphate-buffered saline (PBS) at pH 7.4 (15 mg in 20 mL) with constant stirring for 30 min (at 600 rpm and 25°C). Subsequently, they were centrifuged at 14,000 rpm for 1.5 h at 4°C. The insulin content was then determined using HPLC "Jasco; LC-4000; Tokyo; Japan". The calculation of the insulin amount was performed according to the following formulas [27].

EE (%) = [[Total amount of insulin added − free insulin] / [Total amount of insulin added] × 100.

LC (%) = [[Total amount of insulin added − free insulin]/ weight of nanoparticles] × 100.

2.6. Insulin release assessment

The assessment of insulin release from the encapsulated ILNs-3 was carried out under simulated conditions mimicking gastric fluid (SGF, pH 1.2) and intestinal fluid (SIF, pH 6.8). Initially, 50 mg of ILNs and control (200 mg of insulin alone) were placed into HCl buffer which act as a simulated gastric fluid (SGF) and incubated at 37 °C under constant shaking at 100 rpm for 2 h, followed by incubation in 20 ml of phosphate buffer which as a simulated intestinal fluid (SIF) for an additional 2 hours in triplicate, studied at 37 °C in shaking mode [28]. Subsequently, 2 mL of the released insulin solution was withdrawn at regular intervals, and the volume of each sample was replenished with the same volume of fresh buffer solution simultaneously. The concentration of released insulin was measured using a UV–vis spectrophotometer "Shimadzu, UV-2450, Japan" at 280 nm [29].

2.7. *In Vivo* Pharmacological Activity

The Guidelines for the Care and Use of Laboratory Animals were applied as stated by FELASA (the Federation of European Laboratory Animal Science Association and the European Union (Council Directive 86/609/EEC). Male Wistar rats weighing between 200 and 300 g were kept in controlled environments with temperature kept below 25 °C and relative humidity of 65%. The rats were given unlimited access to tap water and fed a regular diet. The lighting was on a regular cycle of 12 h on and 12 h off. A single intra-peritoneal injection of streptozocin (50 mg/mL in pH 4.5 citrate) at a dose of 50 mg/kg caused rats to develop diabetes. Rats that had fasted blood glucose levels greater than 250 mg/dL after two weeks were employed in the studies. These rats were given free access to water at all times, however they were fasted for 12 h prior to the experiment and for 24 hours during it. Rats were given 1.0 mL of ILNs dispersions intragastrially via gavage needle at a dosage of 50 IU/kg, which was determined by the total amount of insulin present in the ILNs. Equal amounts of insulin oral solution and empty nanocomoposite were given to control rats in a same manner, using the "force-feeding, oral gavage" method, after dissolving bioactive materials in distilled water with 1% (w/v) concentration. Additionally, subcutaneous insulin (2.5 IU/kg) was used as a control. Samples of blood (0.1 mL) were drawn from the tip of the tail vein during 24 h. The relative measure of the cumulative drop in blood glucose levels compared to a 100% availability of the control insulin given subcutaneously at a dose of 2.5 IU/kg was used to calculate the pharmacological availability (PA) of peroral insulin loaded into nanoparticles and in solution. To assess the total amount of insulin delivered to the plasma following insulin injection, plasma insulin levels were plotted against time and the area under the curve was calculated. The Medisense Precision Xceed Kit (Abbot, Portugal) was used to measure the plasma glucose level, which ranged from 10 to 600 mg/dL. The result was expressed as a percentage of the baseline plasma glucose level. The findings are displayed as the average of the values at 6 animals.

2.8. Analytical statistics

Data were attained from triplicated experiments. To perform statistical analyses, the SPSS software package (Version 17.0, SPSS Inc., Chicago, IL) was employed. The triplicate data were averaged, and the significance of the results was assessed using the one-way ANOVA and Student t-test, with a significance threshold set at $p < 0.05$.

3. RESULTS & DISCUSSION

Polymeric nanoparticles have been utilized in research for delivering pharmacological molecules such as insulin due to their exceptional attributes, including biodegradability, biocompatibility, high encapsulation efficiency, cost-effectiveness, high stability, and delayed release effects [30]. Negatively charged polymers and cationic Cht have been shown to electrostatically interact, forming NPs that are employed for loading proteins and peptides such as insulin [31]. Cht and SqM/SeNPs served as carrier polymers in the self-gelation process for the formation of insulin-loaded nanocomposites. Through the electrostatic interaction of negatively charged SqM/SeNPs with cationic Cht, a novel polymer entity with enhanced properties compared to the individual polymers was generated, resulting in the formation of nanocomposites. The preparation process of insulin loaded nanocomposites is illustrated in **Figure 1**.

.

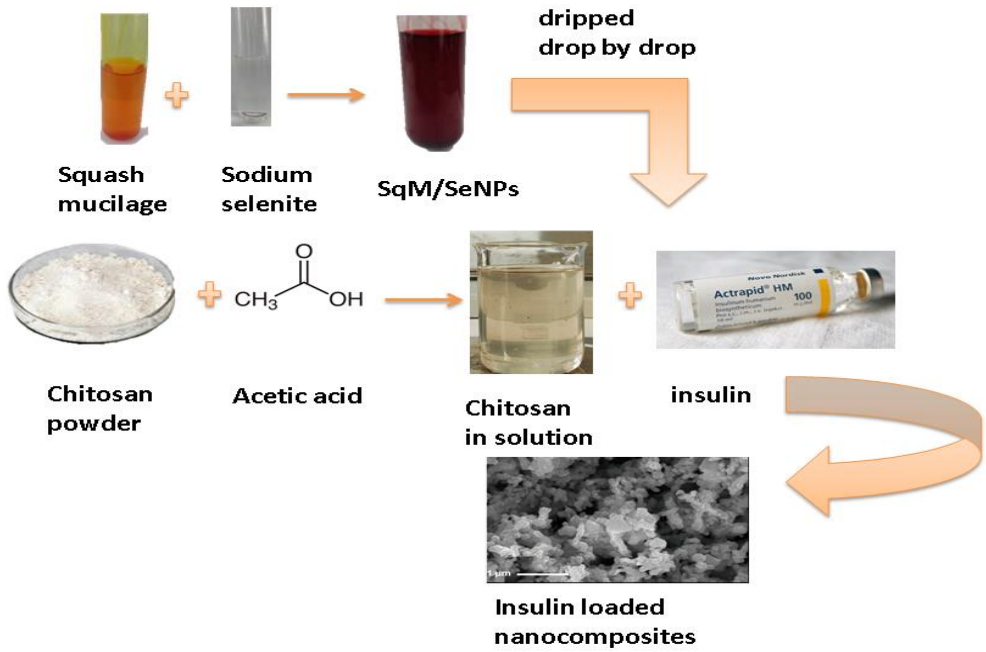

Figure 1: Prepration process of insulin loaded nanocomposites.

3.1. Characterization of Insulin Loaded biopolymer Nanocomposites (ILNs)

3.1.1. Fourier Transform Infrared (FTIR) Spectroscopy

Fourier-transform infrared (FTIR) spectroscopy was employed to analyze the functional groups and molecular interactions present in various samples, including SqM, SqM/SeNPs, insulin, Cht /insulin nanocomposites, and insulin-loaded nanocomposites. The FTIR spectra were carefully examined, and significant changes in the bands were observed. The regions highlighted in red correspond to specific absorption bands identified in SqM, which were attenuated upon conjugation with SeNPs. This suggests that SeNPs may induce the cleavage of certain molecular bonds within the SqM structure. Additionally, new absorption bands, highlighted in blue, emerged in the FTIR spectra after the interaction between SqM and SeNP, indicating the formation of new chemical bonds between SqM and SeNPs. These findings suggest that the conjugation of SeNPs with SqM results in structural modifications, leading to the creation of novel molecular interactions between the components. Chemical interaction between the drug and the nanocarrier was observed, as confirmed by the analysis of FT-IR spectra (**Fig 2**). In the spectral range of 2892–2765 cm^{-1}, SqM exhibits CH absorptions. The absorption bands at 3780–3380 cm^{-1} are attributed to hydroxyl groups (O–H) originating from carbohydrates or other substances such as carboxylic acid and ketones. Bands at 1210–987 cm^{-1} are associated with lipids [32].

The shifts in peaks from 2892 to 3412 cm^{-1} are linked to O–H stretching vibration, and the shifts from 1210 to 1470 cm^{-1} indicate the formation of SqM/SeNPs.Insulin alone exhibited distinct peak at approximately 3250 cm^{-1} (corresponding N–H stretching), 1057 cm^{-1} and 2861 cm^{-1} (associated with C–H stretching), 2705 cm^{-1} (O–H stretch of carboxylic acid), 1622 cm^{-1} (C=O stretching), and 1463 cm^{-1} (aromatic C=C stretching) [27]. The insulin spectrum's peak at 1622 cm^{-1} was altered to 1695 cm^{-1}, and a new peak emerged at 1487 cm^{-1}. The acetylated Cht segment, represented by the 1487 cm^{-1} peak, remained unchanged during the bonding process between the phosphate groups of the anion and the amino groups of the polymer chain at 1695 cm^{-1} [33].

The original distinct absorption peaks of insulin were identified in the FT-IR spectrum of insulin-loaded nanocomposites at approximately 3610 cm^{-1} (O–H stretch of alcohol), 2935 cm^{-1} (C–H stretching), 2613 cm^{-1} and 680 cm^{-1} (O–H stretch of carboxylic acid), and 1750 cm^{-1} (C=O stretching). Based on the spectroscopic results presented above, it can be inferred that the medication and the polymers used to create the NPs are compatible.

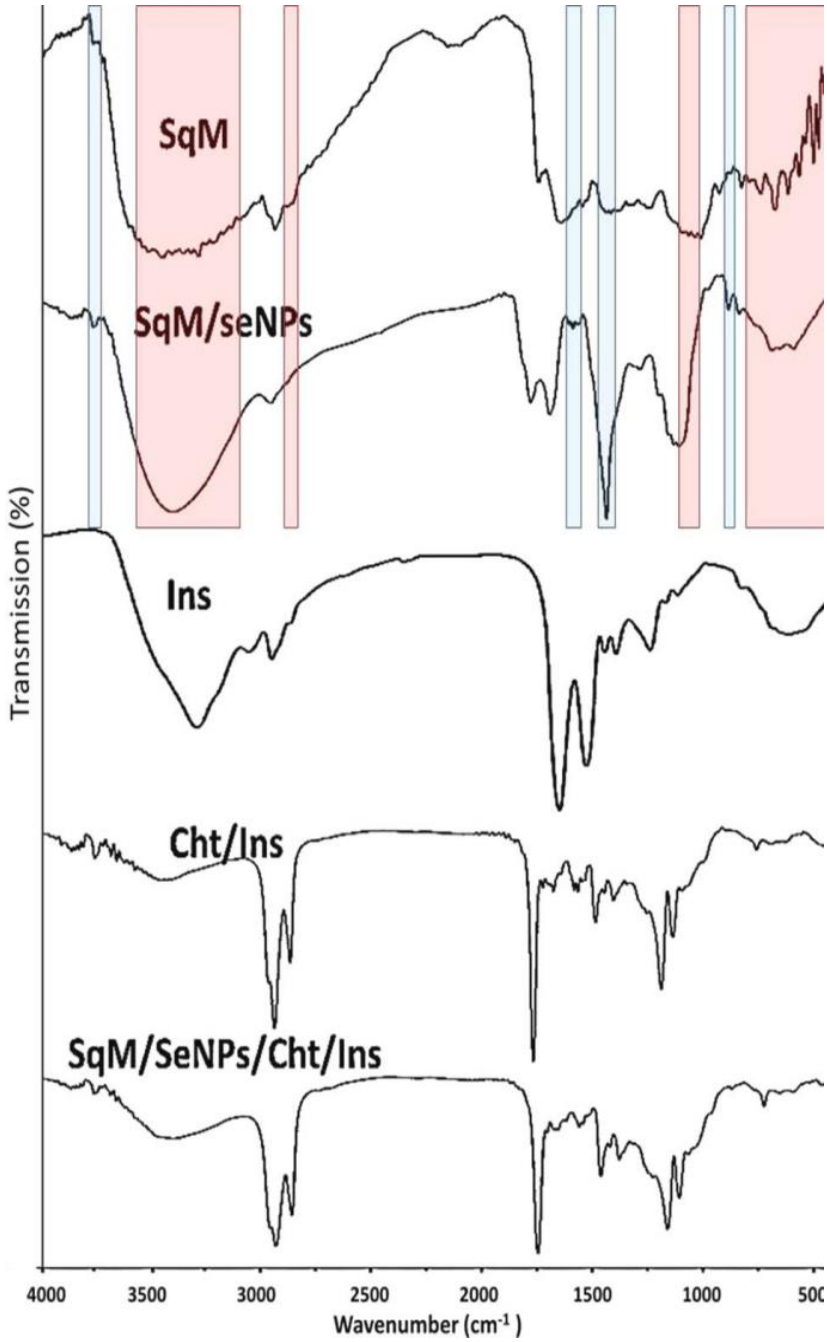

Figure 2: FTIR of squash mucilage, squash mucilage/selenium nanoparticles, insulin, chitosan/insulin nanocomposite and insulin loading nanocomposites.

3.1.2. Zeta Potential (ζ) and particle size (Ps) Analysis

The Ps and ζ potential of the synthesized SqM/SeNPs and ILNs in the study highlight the capability of SqM to produce SeNPs with a mean diameter within a specific Ps range. The ILNs-3 exhibited an average Ps of 308.72 nm, ranging from 95.85-638.42 nm, and displayed substantial positive surface charges (+18.62 mV). Additionally, the phytosynthesized SeNPs demonstrated a negative ζ potential of -28.61 mV. The prevalence of Cht charge over SqM/SeNPs is likely responsible for the positive surface charge observed in the NPs. This indicates that Cht was adsorbed onto the surface of the NPs through ionic interactions with SqM/SeNPs, encapsulating insulin in the core of the particles. Unlike neutral or negatively charged particles, the advantage of positive surface charges is that they can facilitate the smooth passage of NPs through cell membranes. Moreover, the interactions between these positively charged particles and the negatively charged SqM/SeNPs in the gastrointestinal tract may enhance the particles' ability to adhere to the wall, extending the release of the medicine for improved absorption [34].

Table 1: The Particle size distribution and ζ potential of the synthesized SqM/SeNPs, and ILNs at various concentrations.

Sample	Chitosan/Insulin: Mucilage ratio	Particle size range (nm)	Particles size mean (nm)	Zeta potential (mV)
Chitosan	1:0	ND	ND	+35.65 ± 1.45
SqM	0:1	ND	ND	- 29.18 ± 1.09
SqM/SeNPs	0:1	3.12-32.87	13.46±3.52	- 28.61 ± 0.57
ILNs -1	1:2	120.64-794.41	395.93±52.41	- 26.41 ± 0.72
ILNs -2	1:1	84.35-594.41	235.43±34.93	- 11.46 ± 0.65
ILNs -3	2:1	95.85-638.42	308.72±49.66	+18.62 ± 0.86

* ND: not detected

3.1.3. Transmission Electron Microscopy (TEM)

The TEM images in Figure 3 illustrate the distribution and structural characteristics of the synthesized ILNs. The size of nanoparticles significantly impacted both drug release and cellular uptake [27]. The ILNs exhibited a smooth and round shape, with particles displaying an approximately spherical form and diameter sizes consistent with the results obtained from the DLS study. Microscopic SqM/SeNPs particles were evident in the ILNs with Cht/Ins. The observed microscopic sizes of the nanoparticles and their uniform distribution indicate that SqM/SeNP exerted robust reducing and stabilizing effects, leading to the formation of well-defined ILNs.

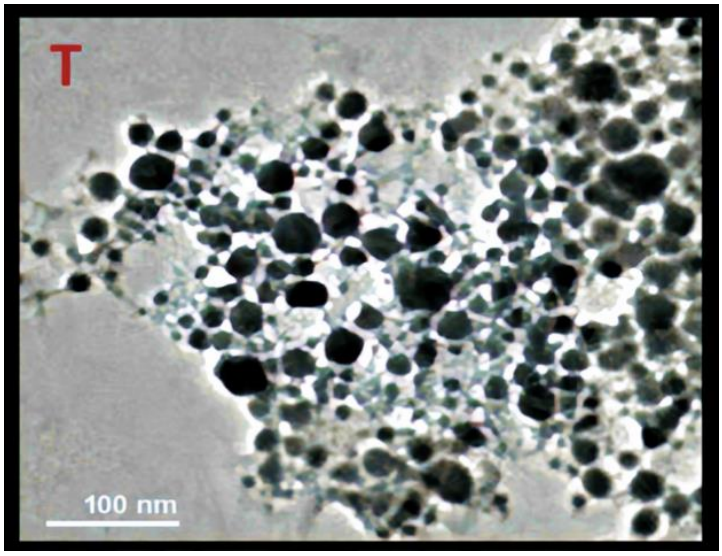

Figure 3: TEM image of synthesized insulin loading biopolymers nanocomposites.

3.1.4. Scanning Electron Microscopy (SEM)

The SEM analysis of the insulin-loaded nanocomposites (ILNs) at different concentrations revealed distinct microstructural characteristics, as shown in Fig. 4. The particles exhibited a smooth, spherical morphology with minimal agglomeration, indicating good dispersion. Among the different concentrations tested, C3 demonstrated the most favorable characteristics, with an average particle size ranging from 95.85 to 638.42 nm. This

particle size range is particularly advantageous, as nanoparticles smaller than 1000 nm are known to enhance pharmacological effects and extend the circulation half-life of the encapsulated drug [35]. In contrast, the C1 formulation, which had a larger particle size distribution, showed more agglomeration and less uniformity. The C3 formulation with its optimal particle size and morphology, showed superior performance over C1 and C2, suggesting that the concentration in C3 provides the best balance between particle size, drug loading, and stability. These findings indicate that C3 is the most promising formulation for improving the therapeutic efficacy of insulin-loaded nanocomposites.

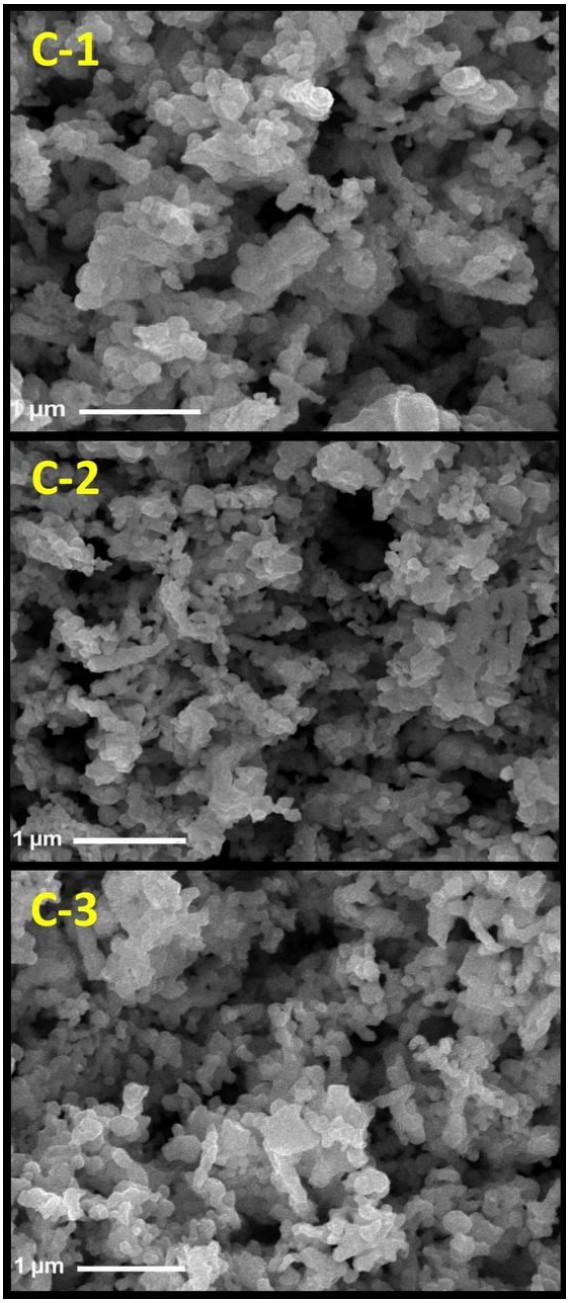

Figure 4: SEM image of synthesized insulin-loading biopolymers nanocomposites at different concentrations of chitosan: squash mucilage/SeNPs with 1:2 (C-1), 1:1 (C-2) and 2:1 (C-3) ratios.

3.2. EE (Encapsulation Efficiency) and LD (Loading Degree) of Insulin

Encapsulation efficiency (EE) and loading capacity (LD) are crucial parameters in drug delivery, and their values are affected by various experimental factors. In the case of the ILNs-3, the encapsulation efficiency and loading capacity were determined to be 75.7% and 4.76%, respectively. **Insulin Release Assessment**

The insulin release characteristics from insulin-loaded nanocomposites (ILNs-3) were investigated under simulated gastrointestinal conditions to understand their potential performance *in vitro*. The release was evaluated at two different pH values, 1.2 (simulating gastric conditions) and 6.8 (mimicking the intestinal environment). After two hours at pH 1.2, approximately 35 % of the total insulin was released, as shown in Fig. 5, while at pH 6.8, a higher release of about 68 % was observed. Notably, the release profile exhibited an initial burst, followed by a slower release phase, which was more pronounced under neutral pH conditions (pH 6.8) compared to acidic conditions (pH 1.2). This suggests that insulin is preferentially released as the formulation progresses through the gastrointestinal tract, especially under intestinal conditions where absorption is more favorable. The differences in release behavior between pH 1.2 and 6.8 indicate that the nanoparticle formulation is sensitive to pH changes, likely due to the role of Cht and (SqM/SeNPs)-modified Cht in the release mechanism. These biopolymers are known to interact with the surrounding environment, where the Cht nanoparticles are more stable in acidic conditions (simulating the stomach) but undergo more significant dissolution and insulin release at higher pH (simulating the small intestine). This gradual release of insulin, especially at neutral pH, enhances the bioavailability and controlled release of the drug, ensuring that insulin is released when absorption rates are at their peak. Furthermore, the stability of the nanoparticles in the gastric environment is crucial for protecting the encapsulated insulin from premature degradation by gastric proteases [36]. The observed controlled release profile and the stability of the nanoparticles in different simulated gastrointestinal fluids suggest that the ILNs formulation has promising potential for oral insulin delivery, offering sustained release and protection against the harsh conditions of the digestive tract.

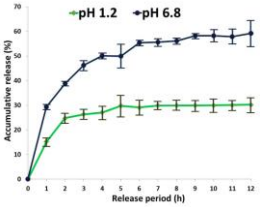

Figure 5: The release of insulin from chitosan/squash mucilage/SeNPs nanocomposite under gastric fluid (SGF) and intestinal fluid (SIF) conditions.

While the individual components of the current study (Cht, SqM, SeNPs, and insulin delivery) are well-established, our approach innovatively combines these elements in a novel way to fabricate innovative natural nanocomposites. The originality of using squash-synthesized SeNPs and their application for insulin delivery through nanoconjugation with Cht provided a promising approach for the hormonal oral delivery.

3.4. *In Vivo* Pharmacological Activity

The diabetic rats after being fasted overnight, the prepared ILNs were given to them. The mean plasma glucose level was evaluated at 100% (Figure 6). Blood glucose level dropped dramatically following the subcutaneous injection of 2.5 IU/Kg insulin solution by 40 % after 1 h, reaching a maximum reduction after 2 h by 57% to confirm the effectiveness of this nano-composite, this results compared with the results obtained after administration of a 50 IU/kg insulin solution.

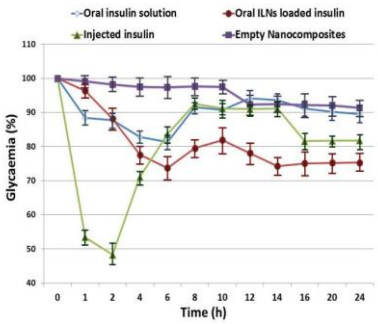

Figure 6 Percentage reduction of plasma glucose concentration in diabetic rats after administration of loaded nanocomposites with insulin at 50 IU/kg, oral insulin solution at 50 IU/kg, subcutaneous injection of insulin at 2.5 IU/kg, and plain nanocomposite*

* Data represents the mean ± SEM, n = 6 per group.

After 6 hrs the blood glucose level was dropped by only less than 15 percent. ILNs lowered blood glucose levels more effectively than rats that received an oral insulin solution or empty nanocomposites (Figure 6). The results validated the effectiveness of ILNs nanocomposite as an oral carrier of insulin, which is mainly attributed to the protective action of Cht and SqM for preventing hormone degradation in the gastrointestinal tract and providing sustained release of hormone into blood circulation [37-42]. The combined actions of ILNs constituents are synergistically strengthened their antidiabetic potentiality, which advocates their practical applications for insulin oral delivery.

4. CONCLUSIONS

Oral absorption of insulin was significantly enhanced through the use of an insulin-loaded biopolymer nanocomposite during oral administration. The combination of pH-sensitive formulation benefits with Cht-based nanoparticulate systems was employed to enhance the oral distribution of peptide medications. The findings demonstrated that incorporating SqM/SeNPs into the formulation significantly improved the acid stability of Cht and their ability to protect encapsulated insulin from stomach degradation. Thus, the pH-sensitive ILNs represent a promising delivery system for the absorption and protection of protein and peptide therapies during oral administration. Furthermore, this approach provides the potential for controlling the drug's release rate and facilitating its passage through the intestinal barrier.

5. Acknowledgements

"The authors would like to thank the Deanship of Scientific Research at Shaqra University, KSA, for supporting this work".

6. References

[1]. C. Y. Wong, H. Al-Salami, C. R. Dass, Recent advancements in oral administration of insulin-loaded liposomal drug delivery systems for diabetes mellitus, International journal of pharmaceutics 549(1-2) (2018) 201-217.

[2]. B. Homayun, X. Lin, H. J. Choi, Challenges and recent progress in oral drug delivery systems for biopharmaceuticals, Pharmaceutics 11(3) (2019) 129.

[3]. A. K. Prusty, S. K. Sahu, Newer approaches for insulin administration in diabetes treatment, Pharmacologyonline 2 (2009) 852-861.

[4]. F. Cui, K. Shi, L. Zhang, A. Tao, Y. Kawashima, Biodegradable nanoparticles loaded with insulin–phospholipid complex for oral delivery: preparation, in vitro characterization and in vivo evaluation, Journal of controlled release 114(2) (2006) 242-250.

[5]. S. Salar, M. Jafari, S. F. Kaboli, F. Mehrnejad, The role of intermolecular interactions on the encapsulation of human insulin into the chitosan and cholesterol-grafted chitosan polymers, Carbohydrate polymers 208 (2019) 345-355.

[6]. C. P. Reis, C. Damgé, Nanotechnology as a promising strategy for alternative routes of insulin delivery. Methods in enzymology 508 (2012) 271-294.

[7]. F. Bahman, K. Greish, S. Taurin, Nanotechnology in insulin delivery for management of diabetes, Pharmaceutical nanotechnology 7(2) (2019) 113-128.

[8]. S. Bakand, A. Hayes, F. Dechsakulthorn, Nanoparticles: a review of particle toxicology following inhalation exposure, Inhalation toxicology, 24(2) (2012) 125-135.

[9]. H., Abbas, D. Abou Baker, Biological evaluation of selenium nanoparticles biosynthesized by Fusarium semitectum as antimicrobial and anticancer agents. Egyptian Journal of Chemistry, 63(4) (2020) 1119-1133. DOI: 10.21608/ejchem.2019.15618.1945

[10]. M. Kieliszek, S. Błażejak, Current knowledge on the importance of selenium in food for living organisms: a review, Molecules 21 (5) (2016) 609.

[11]. A. ELMESALLAMY, M. El-Zaidy, M. Younes, S. A. A. Hussein, Green Biosynthesized Selenium Nanoparticles and Bioactive Compounds by Gossypium barbadense L Extract and Their Cytotoxic Potential. *Egyptian Journal of Chemistry*, *66*(8) (2023) 439-448. DOI: 10.21608/ejchem.2022.171646.7132

[12]. B. T. Abduljabbara, M. M. El-Zayat, E. S. F. El-Halawany, Y. A. El-Amier, Selenium nanoparticles from Euphorbia retusa extract and its biological applications: antioxidant, and antimicrobial activities. *Egyptian Journal of Chemistry*, *67*(2) (2024) 463-472. DOI: 10.21608/EJCHEM.2023.214819.8069

[13]. M. P. Rayman, K. H. Winther, R. Pastor-Barriuso, F. Cold, M. Thvilum, S. Stranges, S. Cold, Effect of long-term selenium supplementation on mortality: results from a multiple-dose, randomised controlled trial, Free Radical Biology and Medicine 127 (2018) 46-54.

[14]. M. Wahba, Recent Insights on Chitosan's Applications. Egyptian Journal of Chemistry, 63(4) (2020) 1179-1204. DOI: 10.21608/ejchem.2019.12353.1770

[15]. H. S. AlSalem, N. M. Abdulsalam, N. A. Khateeb, M. S. Binkadem, N. A. Alhadhrami, A. M. Khedr, E. H. Nadwa, Enhance the oral insulin delivery route using a modified chitosan-based formulation fabricated by microwave, International Journal of Biological Macromolecules 247 (2023)125779.

[16]. C. M. Lehr, J. A. Bouwstra, E. H. Schacht, H. E. Junginger, In vitro evaluation of mucoadhesive properties of chitosan and some other natural polymers, International journal of Pharmaceutics 78(1-3) (1992) 43-48.

[17]. S. K. Sahu, Development and evaluation of insulin incorporated nanoparticles for oral administration, International Scholarly Research Notices (2013*) 2013*.

[18]. A. Hussain, T. Kausar, A. Din, M. A. Murtaza, M. A. Jamil, S. Noreen, M. A. Ramzan, Determination of total phenolic, flavonoid, carotenoid, and mineral contents in peel, flesh, and seeds of pumpkin (Cucurbita maxima), Journal of Food Processing and Preservation 45(6) (2021) e15542.

[19]. F. Li, Y. Wei, J. Zhao, L. Zhang, Q. Li, In vivo pharmacokinetic study of a Cucurbita moschata polysaccharide after oral administration, International Journal of Biological Macromolecules 203(2022) 19-28.

[20]. A. S. Talab, A. Hussein, M. M. Kamil, S. Mostafa, N. A. Hegazy, K. F. Mahmoud, Synthesis and Characterization of Chitosan Nanoparticles from some Crustacean Wastes. Egyptian Journal of Chemistry, 67(5) (2024) 23-42. DOI: 10.21608/ejchem.2023.228113.8401

[21]. K. Pyrzynska, A. Sentkowska, Biosynthesis of selenium nanoparticles using plant extracts, Journal of Nanostructure in Chemistry (2021) 1-14.

[22]. L. Huang, J. Zhao, Y. Wei, G. Yu, F. Li, Q. Li, Structural characterization and mechanisms of macrophage immunomodulatory activity of a pectic polysaccharide from Cucurbita moschata Duch, Carbohydrate polymers 269 (2021). 118288.

[23]. M. M. Tosif, A. Najda, A. Bains, R. Kaushik, S. B. Dhull, P. Chawla, M. Walasek-Janusz, A comprehensive review on plant-derived mucilage: characterization, functional properties, applications, and its utilization for nanocarrier fabrication, Polymers 13(7) (2021). 1066.

[24]. I. Saha, S. Roy, D. Das, S. Das, P. Karmakar, Topical effect of polyherbal flowers extract on xanthan gum hydrogel patch—induced wound healing activity in human cell lines and male BALB/c mice, Biomedical Materials 18(3) (2023) 035016.

[25]. W. A. Abd-Elraoof, A. A. Tayel, S.W. El-Far, O. M. W. Abukhatwah, A. M. Diab, O. M. Abonama, M. A. Assas, A. Abdella, Characterization and antimicrobial activity of chitosan-selenium nanocomposite biosynthesized using Posidonia oceanica. RSC Advances. 13 (2023) 26001-26014. https://doi.org/10.1039/D3RA04288J

[26]. H. A. Gad, A. A. Tayel, M. S. Al-Saggaf, S. H. Moussa, A. M. Diab, Phyto-fabrication of selenium nanorods using extract of pomegranate rind wastes and their potentialities for inhibiting fish-borne pathogens, Green Processing and Synthesis 10(1) (2021). 529-537.

[27]. M. Li, Y. Sun, C. Ma, Y. Hua, L. Zhang, J. Shen, Design and investigation of penetrating mechanism of octaarginine-modified alginate nanoparticles for improving intestinal insulin delivery, Journal of Pharmaceutical Sciences 110(1) (2021). 268-279.

[28]. N. Dwivedi, M. A. Arunagirinathan, S. Sharma, J. Bellare, Silica-coated liposomes for insulin delivery, *Journal of Nanomaterials* 2010 (2010) 1-8.

[29]. Y. Yang, Y. Liu, S. Chen, K. L. Cheong, B. Teng, Carboxymethyl β-cyclodextrin grafted carboxymethyl chitosan hydrogel-based microparticles for oral insulin delivery, Carbohydrate polymers 246 (2020) 116617.

[30]. M. A. Mumuni, F. C. Kenechukwu, K. C. Ofokansi, A. A. Attama, D. D. Díaz, Insulin-loaded mucoadhesive nanoparticles based on mucin-chitosan complexes for oral delivery and diabetes treatment, Carbohydrate polymers 229 (2020)115506.

[31]. M. E. S. Hassan, J. Bai, D. Q. Dou, Biopolymers; definition, classification and applications. Egyptian Journal of Chemistry, 62(9) (2019) 1725-1737.

[32]. A. W. Indrianingsih, W. Apriyana, K. Nisa, V. T. Rosyida, S. N. Hayati, C. Darsih, A. Kusumaningrum, Antiradical activity and physico-chemical analysis of crackers from cucurbita moschata and modified cassava flour, Food Research 3(5) (2019) 484-490.

[33]. Y. Xu, Y. Du, Effect of molecular structure of chitosan on protein delivery properties of chitosan nanoparticles, International journal of pharmaceutics 250(1) (2003) 215-226.

[34]. T. Moschakis, B. S. Murray, C. G. Biliaderis, Modifications in stability and structure of whey protein-coated o/w emulsions by interacting chitosan and gum arabic mixed dispersions, Food Hydrocolloids 24(1) (2010) 8-17.

[35]. X. Xue, S. Raynard, V. Busygina, A. K. Singh, P. Sung, Role of replication protein A in double holliday junction dissolution mediated by the BLM-Topo IIIα-RMI1-RMI2 protein complex, Journal of Biological Chemistry 288(20) (2013) 14221-14227.

[36]. E. B. Souto, S. B. Souto, J. R. Campos, P. Severino, T. N. Pashirova, L. Y. Zakharova, A. M. Silva, A. Durazzo, M. Lucarini, A. A. Izzo, A. Santini, Nanoparticle Delivery Systems in the Treatment of Diabetes Complications, Molecules (Basel, Switzerland) 24(23) (2019) 4209. https://doi.org/10.3390/molecules24234209

[37]. R. M. Salama, H. Osman, H. M. Ibrahim, Preparation of biocompatible chitosan nanoparticles loaded with *Aloe vera* extract for use as a novel drug delivery mechanism to improve the antibacterial characteristics of cellulose-

based fabrics. Egyptian Journal of Chemistry, 65(3) (2022) 589-604. https://doi.org/10.21608/ejchem.2021.96434.4512

[38]. A. E. Abdelhamid, A. A. El-Sayed, S. A. Swelam, A. M. Soliman, A. M. Khalil, Encapsulation of Triazole Derivatives Conjugated with Selenium Nanoparticles onto Nano-Chitosan for Antiproliferative Activity towards Cancer Cells. Egyptian Journal of Chemistry. 65(131) (2022) 1231-1239. https://doi.org/10.21608/ejchem.2022.147872.6401

[39]. E. T. Amer, A. A. Tayel, A. I. Abd El Maksoud, M. Alsieni, H. A. Gad, M. A. Assas, A. Abdella, D. Elebeedy Antibacterial Potentialities of Chitosan Nanoparticles Loaded with Salvianolic Acid B and Tanshinone IIA. BioNanoScience. 14 (2023) 594–604. https://doi.org/10.1007/s12668-023-01263-2

[40]. E. M. Meshref, A. A. E.-D. Omar, S. H. Moussa, A. H. Alabdalall, M. S. Al-Saggaf, A. I. Alalawy, F. M. Almutairi, H. A. Gad, A. A. Tayel, Antimicrobial Nanocomposites from Chitosan and Squash Synthesized Nano-Selenium Eradicate Skin Pathogens. ChemistrySelect. (2024). https://doi.org/10.1002/slct.202400881

[41]. M.M. El-Sherbiny, M.E. El-Hefnawy, A.A. Tayel, Innovative anticancer nanocomposites from Corchorus olitorius mucilage/chitosan/selenium nanoparticles. International Journal of Biological Macromolecules. 282,(2024)137320. https://doi.org/10.1016/j.ijbiomac.2024.137320

[42]. A. A. S. Aborabu, A. A. Tayel, M. A. Assas, S. H. Moussa, A. I. Alalawy, F. M. Almutairi, A. AE-D Omar, Anti-Helicobacter pylori activity of nanocomposites from chitosan/broccoli mucilage/selenium nanoparticles. Scientific Reports. 14 (2024) 21693. https://doi.org/10.1038/s41598-024-65762-2